Electronic Supplementary Information for

Sb@C coaxial nanotubes as superior long-life and high-rate anode for sodium ion batteries

Zhiming Liu,[a‡] Xin-Yao Yu,[ab‡] Xiong Wen (David) Lou[bc] and Ungyu Paik*[a]*

[a] Department of Energy Engineering, Hanyang University, 222 Wangsimni-ro, Seongdong-gu, Seoul, 04763, Korea E-mail: upaik@hanyang.ac.kr

[b] State Key Laboratory of Silicon Materials, School of Materials Science and Engineering, Zhejiang University, Hangzhou, 310027, P. R. China Email: davidlou88@gmail.com

[c] School of Chemical and Biomedical Engineering, Nanyang Technological University, 62 Nanyang Drive, Singapore 637459, Singapore E-mail: xwlou@ntu.edu.sg

[‡] These authors contributed equally to this work.

Experimental Section

Synthesis of Sb_2S_3 nanorods: The Sb_2S_3 nanorods were synthesized through a simple hydrothermal method. In a typical synthesis, 4 mmol of $SbCl_3$, 8 mmol of L-cysteine, and 8 mmol of $Na_2S \cdot 9H_2O$ were orderly dissolved in 80 mL of distilled water (DIW) under stirring for 3 h to form a homogeneous suspension. Afterwards, the above solution was transferred into a 100 mL Teflon-lined stainless steel autoclave and then kept at 180 ℃ for 12 h. After cooling down to room temperature naturally, the obtained dark-brown product was separated by centrifugation, washed with DIW and ethanol for several time before drying at 60 ℃ overnight under vacuum.

Synthesis of Sb_2S_3@PDA core-shelled nanorods: 30 mg of Sb_2S_3 nanorods and 40 mg of dopamine hydrochloride were dispersed into 100 mL of Tris-buffer solution (10 mM) with sonication for 10 minutes and then magnetic-stirring for 3 h. The resultant product was collected via centrifugation and washed with DIW and ethanol for three times, respectively, and dried at 60 ℃ overnight under vacuum.

Synthesis of Sb@C coaxial nanotubes: Sb_2S_3 nanorods were annealed at 500 ^oC for 1 h in Ar with a heating rate of 3 ^oC min^{-1}. The as-prepared Sb_2S_3@PDA core-shelled nanorods were annealed at 500 ^oC in Ar with a heating rate of 3 ^oC min^{-1} for 2, 5, 20, and 40 min, respectively. After different annealing time, Sb_2S_3@PDA core-shelled nanorods are transformed into Sb@C doble-walled nanotubes.

Materials characterization: Field-emission scanning electron microscope (FESEM; JEOL JSM07600F) and transmission electron microscope (TEM; JEOL JEM-2100F) were used to characterize the microscopic features of the samples. A Rigaku D/MAX RINT-2000 X-Ray Diffractometer with Cu Kα radiation at a voltage of 40 kV and a current of 40 mA was used to collect the XRD patterns of the products. Thermogravimetric analysis (TGA) was performed with a temperature ramp of 10 ^oC min^{-1} under air flow.

Electrochemical measurements: The battery tests were carried out in a half-cell configuration. The working electrode consists of active materials, conductivity agent (Carbon black, CB), and binder (Carboxymethylcellulose sodium, CMC-Na) with a weight ratio of 70:20:10. The mass loading of active materials was about 0.9 mg. The electrolyte was a solution of 1.0 M $NaClO_4$ in propylene carbonate with 5% fluoroethylene carbonate (FEC) additive. Sodium metal was used as both the counter electrode and reference electrode. The coin-type half cells were assembled in argon-filled glovebox and then tested in TOSCAT 3000 battery tester (TOSCAT 3000, Toyo Systems, Tokyo, Japan) with a voltage range between 0.01 and 2.0 V. Cyclic Voltammetry (CV) curves were tested using AUTOLAB potentiostat/galvanostat apparatus (AUT85698) with a scan rate of 0.1 mV s^{-1}.

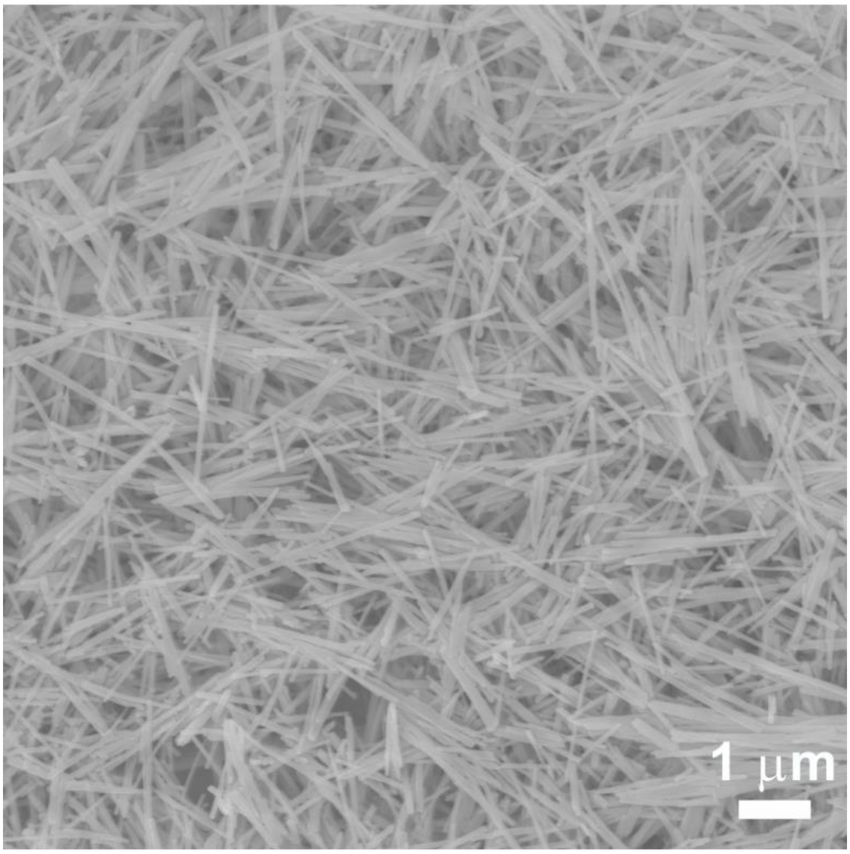

Fig. S1 FESEM image of Sb_2S_3 nanorods.

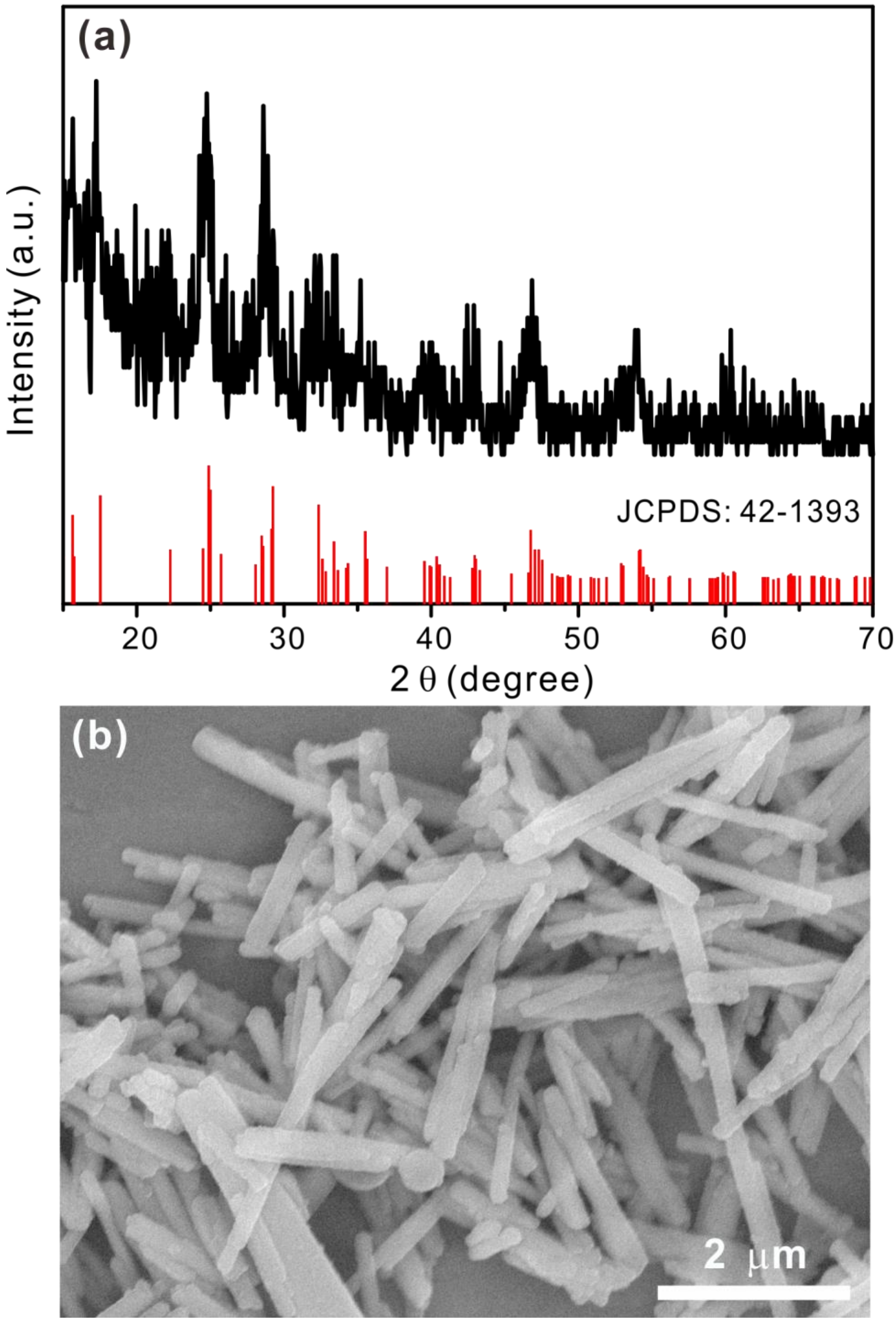

Fig. S2 XRD pattern and FESEM image of Sb_2S_3@PDA core-shell nanorods.

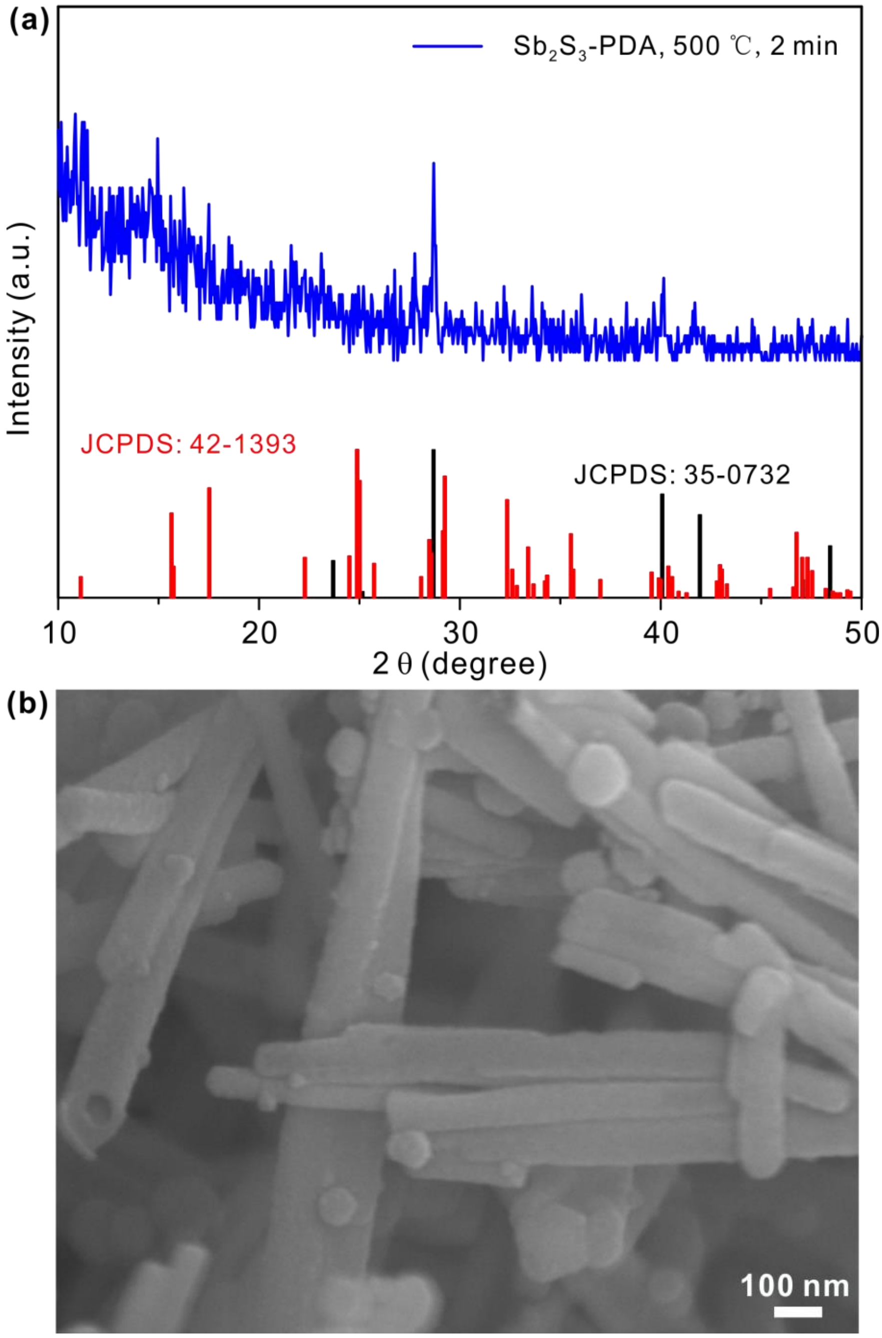

Fig. S3 XRD pattern (a) and FESEM image (b) of Sb_2S_3@PDA-2.

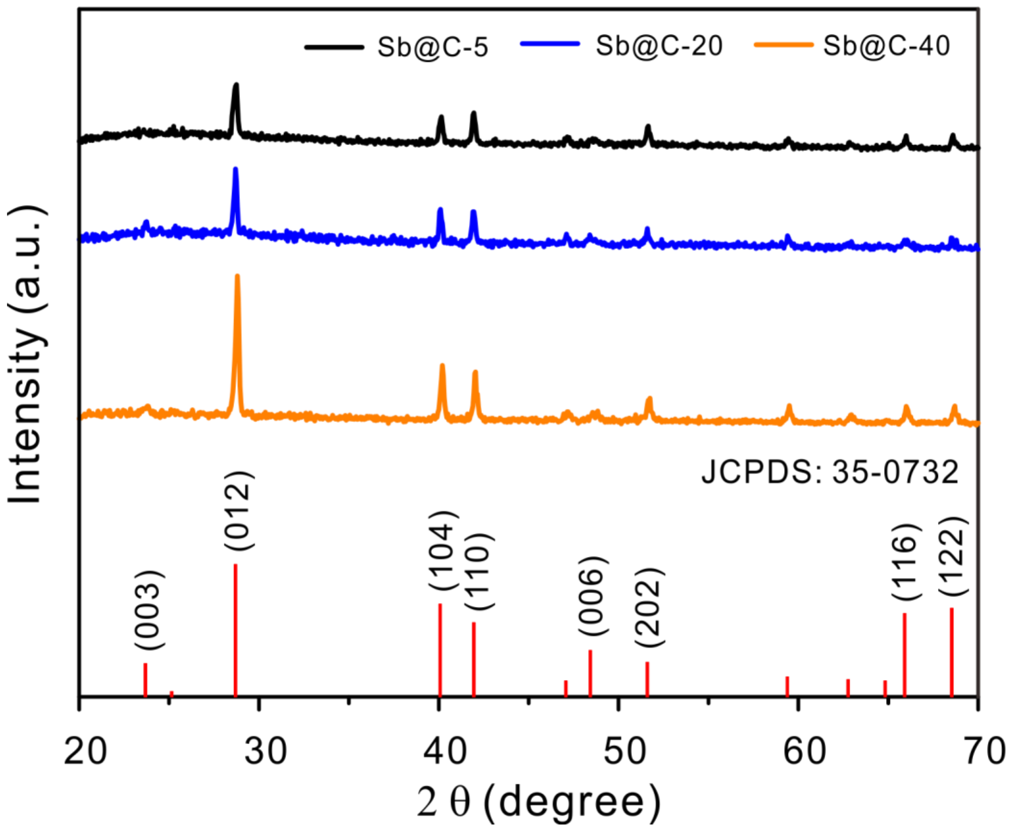

Fig. S4 XRD patterns of Sb@C-5, Sb@C-20, and Sb@C-40.

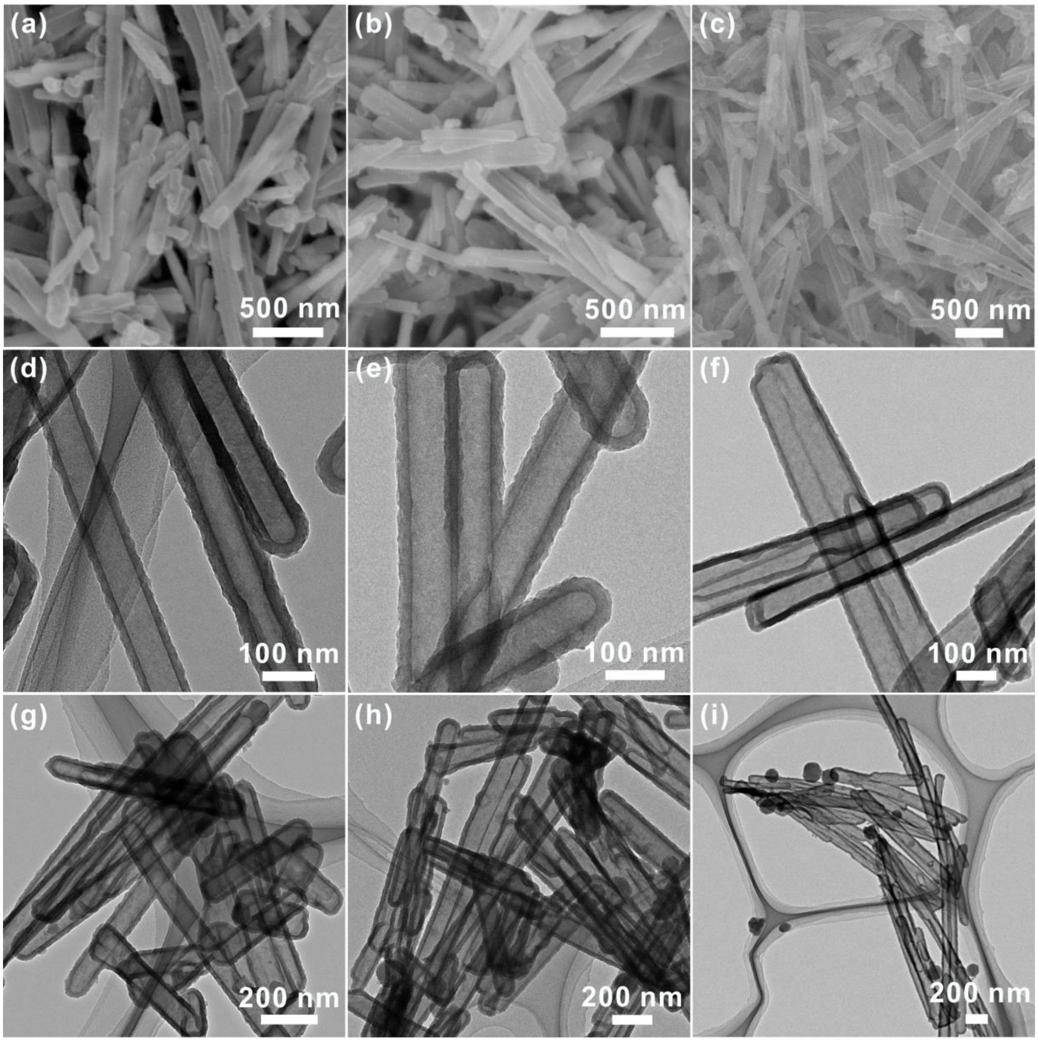

Fig. S5 FESEM (a, b, c) and TEM (c, e, f, g, h, i) images of Sb@C-5 (a, d, g), Sb@C-20 (b, e, h), and Sb@C-40 (c, f, i).

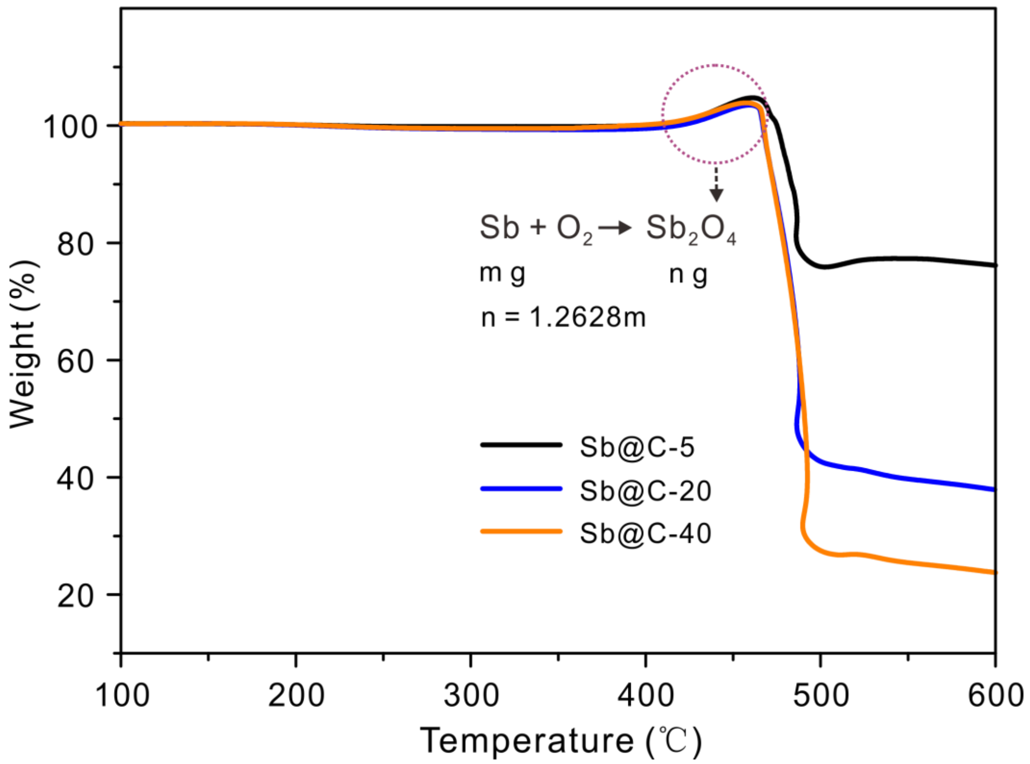

Fig. S6 TGA analysis of Sb@C coaxial nanotubes at a temperature ramp of 10 ^{o}C min^{-1} in air.

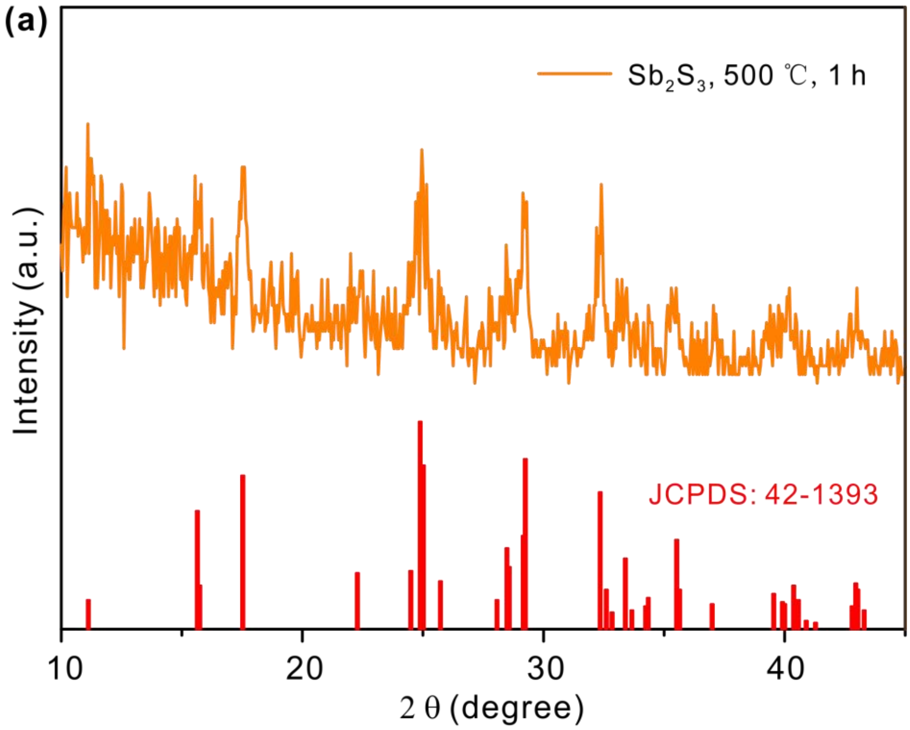

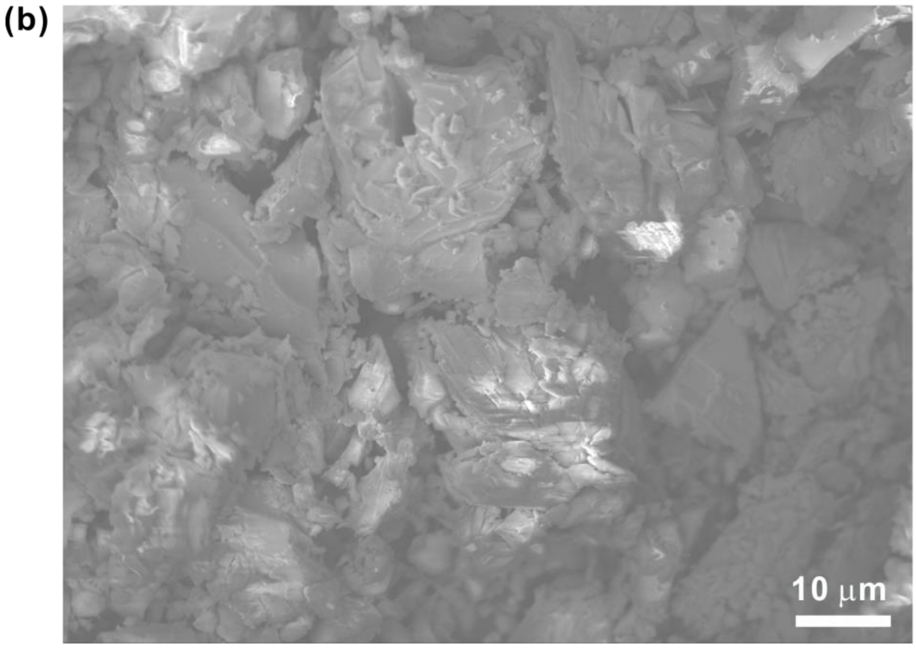

Fig. S7 XRD pattern and FESEM image of Sb_2S_3 nanorods after annealing at 500 ℃ for 1 h in Ar.

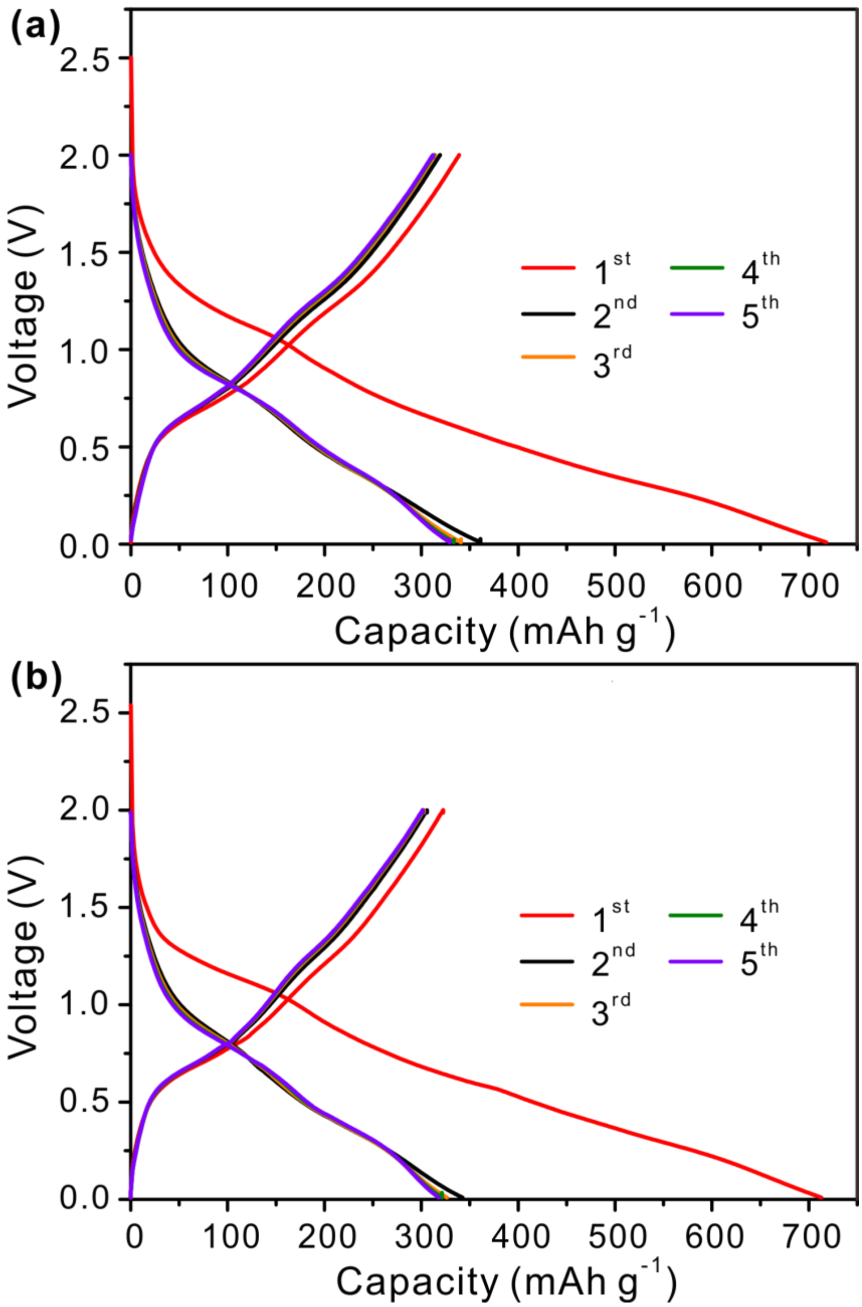

Fig. S8 Charge-discharge voltage profiles of Sb@C-20 (a) and Sb@C-40 (b) for the first five cycles at a current density of 100 mA g^{-1}.

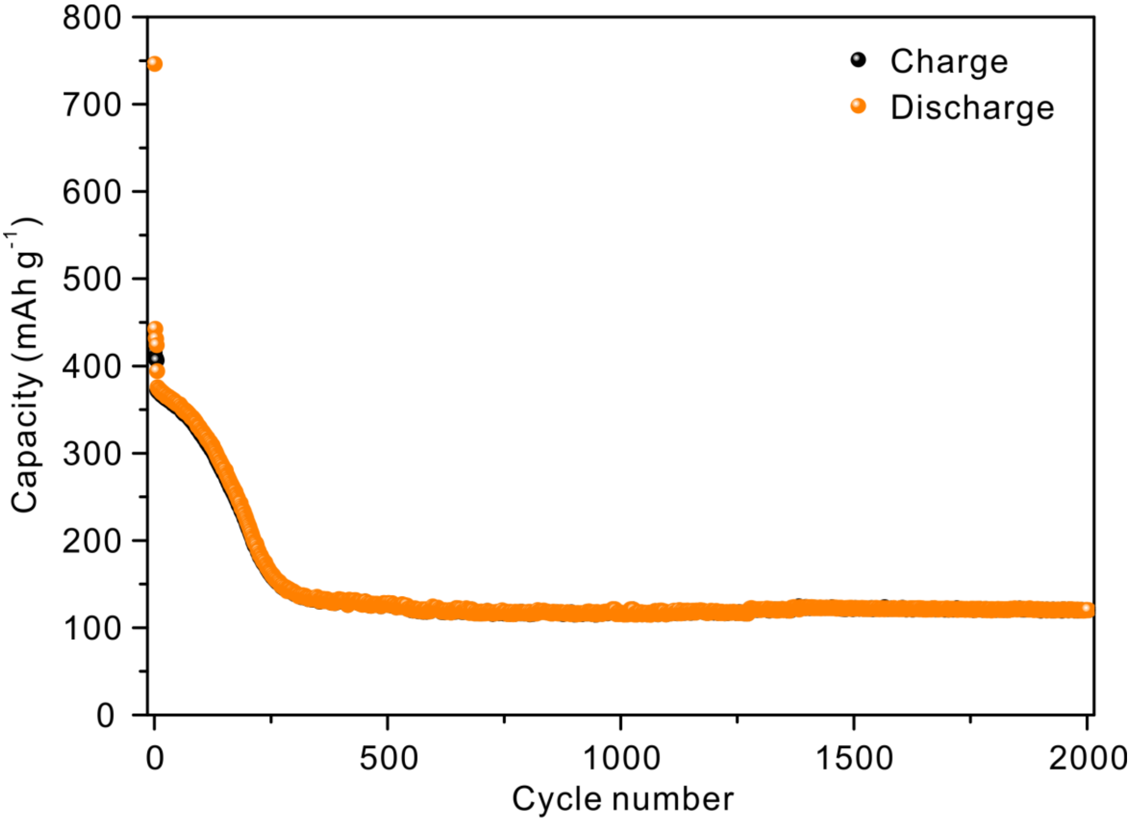

Fig. S9 Cycling performance of Sb_2S_3@PDA-2 at a current density of 1.0 A g^{-1}.

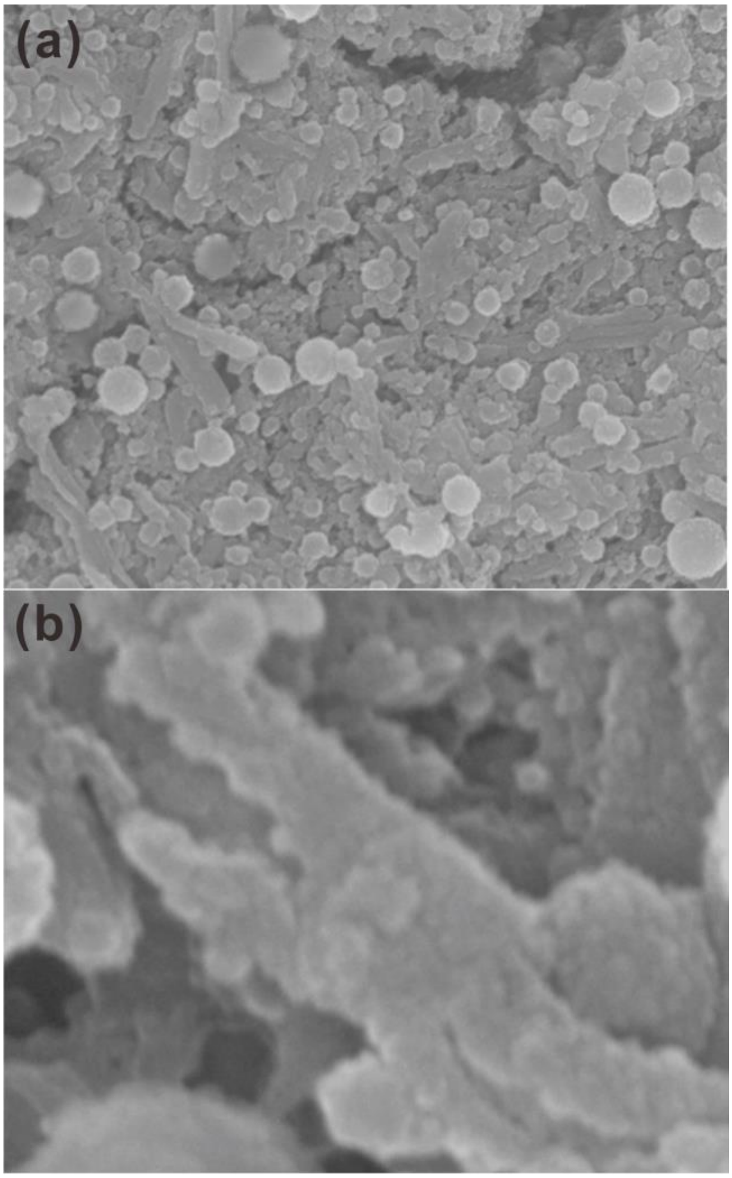

Fig. S10 FESEM images of Sb@C-5 after 2000 cycles at a current density of 1.0 A g^{-1}.

Table S1. Comparison of some representative Sb-based anode materials for SIBs.

Sb-based anodes	**Cycling performance**	**Rate capability**	**Ref.**
Sb nanoparticles decorated N-rich carbon nanosheets	305 mAh g^{-1} after 60 cycles at 50 mA g^{-1}	142 mAh g^{-1} at 10 A g^{-1}	[1]
Sb/C nanofibers	350 mAh g^{-1} after 300 cycles at 100 mA g^{-1}	88 mAh g^{-1} at 6 A g^{-1}	[2]
Sb-C nanofibers	385 mAh g^{-1} after 500 cycles at 100 mA g^{-1}	337 mAh g^{-1} at 3 A g^{-1}	[3]
Sb hollow nanosphere	622.2 mAh g^{-1} after 50 cycles at 50 mA g^{-1}	315 mAh g^{-1} at 1.6 A g^{-1}	[4]
Sb porous hollow microspheres	574 mAh g^{-1} after 100 cycles at 660 mA g^{-1}	313 mAh g^{-1} at 3.2 A g^{-1}	[5]
Spherical nano-Sb@C composite	385 mAh g^{-1} after 500 cycles at 100 mA g^{-1}	270 mAh g^{-1} at 4 A g^{-1}	[6]
Sb/Multilayer Graphene hybrid	405 mAh g^{-1} after 200 cycles at 100 mA g^{-1}	210 mAh g^{-1} at 5 A g^{-1}	[7]
Sb/MWCNT nanocomposite	380 mAh g^{-1} after 120 cycles at 200 mA g^{-1}	225 mAh g^{-1} at 2 A g^{-1}	[8]
Sb @C coaxial nanotubes	407 mAh g^{-1} after 240 cycles at 100 mA g^{-1}	460 mAh g^{-1} at 100 mA g^{-1}	Present work
		350 mAh g^{-1} at 10 A g^{-1}	
	230 mAh g^{-1} after 2000 cycles at 1 A g^{-1}	310 mAh g^{-1} at 20 A g^{-1}	

References

[1] X. Zhou, Y. Zhong, M. Yang, M. Hu, J. Wei, Z. Zhou, *Chem. Commun.* **2014**, *50*, 12888-12891.

[2] Y. Zhu, X. Han, Y. Xu, Y. Liu, S. Zheng, K. Xu, L. Hu, C. Wang, *ACS Nano* **2013**, *7*, 6378-6386.

[3] L. Wu, X. Hu, J. Qian, F. Pei, F. Wu, R. Mao, X. Ai, H. Yang, Y. Cao, *Energy Environ. Sci.* **2014**, *7*, 323-328.

[4] H. Hou, M. Jing, Y. Yang, Y. Zhu, L. Fang, W. Song, C. Pan, X. Yang, X. Ji, *ACS Appl. Mater. Interfaces* **2014**, *6*, 16189-16196.

[5] H. Hou, M. Jing, Y. Yang, Y. Zhang, Y. Zhu, W. Song, X. Yang, X. Ji, *J. Mater. Chem. A* **2015**, *3*, 2971-2977.

[6] N. Zhang, Y. Liu, Y. Lu, X. Han, F. Cheng, J. Chen, *Nano Research* **2015**, *8*, 3384-3393.
[7] L. Hu, X. Zhu, Y. Du, Y. Li, X. Zhou, J. Bao, *Chem. Mater.* **2015**, *27*, 8138-8145.
[8] X. Zhou, Z. Dai, J. Bao, Y.-G. Guo, *J. Mater. Chem. A* **2013**, *1*, 13727.